Available online www.ejaet.com

European Journal of Advances in Engineering and Technology, 2024, 11(12):14-26

Research Article ISSN: 2394 - 658X

Comparative Study of the Microstructural, Mechanical and Tribological behavior of blended Mo-Mo_2C Composite coatings using Atmospheric Plasma Spraying

Muhammad Irfan[1], Badaruddin Soomro[2], Rashid Iqbal[3], M. Usman Tahir[4]

[1,2,3]Pakistan Institute of Technology for Minerals & Advanced Engineering Materials (PITMAEM),
[4]Electrical Measurement & Testing Laboratory (EMTL),
Pakistan Council of Scientific & Industrial Research Laboratories Complex, Ferozepur Road, Lahore-Pakistan-54600
Corresponding author: irfan.pcsir72@gmail.com[1]
Contributing authors: badar.soomro@hotmail.com[2], Rashid.iqbal787@gmail.com[3], hafizusmantahir@hotmail.com[4]

ABSTRACT

Wear and friction are considered as a significant problem in many real-world industries including automobile, aerospace, pulp, paper etc. The present research work based on Synthesis and characterization of blended Mo-Mo_2C composite coatings produced by a systematic combination of Mo_2C powders in pure Mo powder with four percentages: 10%, 20%, 30% and 40% at a constant standoff distance of 100 mm using atmospheric plasma spraying system on AISI 5120 substrate. The resulting blended composite coatings were characterized by SEM, XRD and Tribometer. The results correlate the effect of percentage variations of Mo_2C in pure Mo on tribological behavior of blended Mo-Mo_2C composite coatings with the formation of different microstructural phases, their crystallite sizes, residual stresses, and the resulting mechanical properties.

Keywords: Wear and friction, Standoff distance, Atmospheric plasma spraying, Crystallite sizes, Residual stresses

INTRODUCTION

In machines, various engineering components undergo sliding movement. For example, in components of power generation, boilers, textiles and aerospace but specifically in automobiles in which most of the engine parts are undergoing through sliding movement like piston rings, synchronizing rings etc. During this sliding movement, degradation of surfaces of the engineering components occurs due to the problem of wear and friction in sliding parts of the machines. As a consequence, life of components reduces which ultimately increases the cost of automobile parts. Therefore, wear and friction is considered as a fundamental and important problem in many auto parts. This study aims to address the problem of wear and friction for automobile parts which undergo sliding movement.

Various techniques of surface engineering are available to deposit the preferred protective layers which can reduce the wear and friction in sliding parts e.g. Physical Vapor Deposition (PVD) technique, Plasma Assisted PVD technique, Chemical Vapor Deposition (CVD) technique and Thermal Spraying techniques. Among various surface engineering techniques, Thermal Spray techniques are widely and extensively used for the deposition of various protective coatings like thermal barrier coatings, cermet, composites to enhance the surface properties of the substrate materials [2, 3]. For the automobile industry (which is the focus of this study), atmospheric plasma spraying process is most extensively applied [4-6]. Therefore, this study aims to use the atmospheric plasma spraying process for coatings.

In recent years, pure Molybdenum (Mo) coating has attracted the attentions of research community to produce blended coatings with an aim to enhance the wear and friction properties of coatings. The reason for this is that pure Mo has got excellent properties of scuffing resistance to abrasive wear, as well as high corrosion resistance [7–9]. However, pure Mo coatings show poor resistance to embrittlement, when applied to automobile parts like piston rings [10], cylinder bores [4], synchronizer rings [10-12] etc. To overcome the limitations of pure Mo coatings, researchers have

focused on blending different powders in pure Mo. In this regard, many materials are being used for blending of Mo coatings to improve wear resistance such as bronze, brass, MoSi2, NiCrBSi, Mo_2C and TiN etc. [13-16].
Considering blended Mo-Mo_2C coatings, Liao et al. [17] investigated the structure property relationship of Mo-Mo_2C system. He explained the limitations of pure Mo that it forms a low melting and highly volatile oxides when exposed to temperature above 1063 K. This condition may be improved by blending of Mo_2C. Sampath and Wayne [18] studied the microstructures and friction properties of plasma sprayed Mo-Mo_2C composite coatings. They concluded that softness of plasma sprayed pure Molybdenum coatings can be improved by dispersion strengthening of molybdenum carbide (Mo_2C). As, the wear and friction properties of Mo-Mo_2C composite coatings are dependent on the homogeneous distribution of Mo_2C within the molybdenum matrix. Detailed studies show that wear properties of Mo coatings may be enhanced by blending or dispersion of chromium carbides, molybdenum carbides, or molybdenum oxides etc. [18, 19].
The main aim of this research work is to produce systematic combinations of blended Mo-Mo_2C composite coatings and to study their wear and friction mechanism in correlation with microstructural and mechanical properties.

EXPERIMENTAL SETUP

This section presents the experimental setup used for this study including spray powders used for blended Mo-Mo_2C coatings, substrate and its preparation method, atmospheric plasma spraying system used for spraying and characterization methods used to evaluate the quality of Mo-Mo_2C blended coatings.

Spray powders

Two spray powders are used to synthesis four combinations of blended Mo-Mo_2C composite coatings: (1) pure Mo powder and (2) Mo_2C powder manufactured by H.C. Starck, Germany having particle sizes in a range from 45 to 75 µm to obtain high-density coatings by increasing flow ability of powders inside the plasma jet stream. The morphological structure of these spray powders shows same regular morphology (see Fig. 1(a) & (b)). As the particle size, shape, distribution, and microstructure of these powders mainly depend on their fabrication technique [20].
Pure Mo powder with four percentages; 10%, 20%, 30% and 40% of Mo_2C powders were mechanically mixed using a turbulent shake mixer at a revolving speed of 42 rpm for 20 hrs.in order to obtain uniform blended powders.

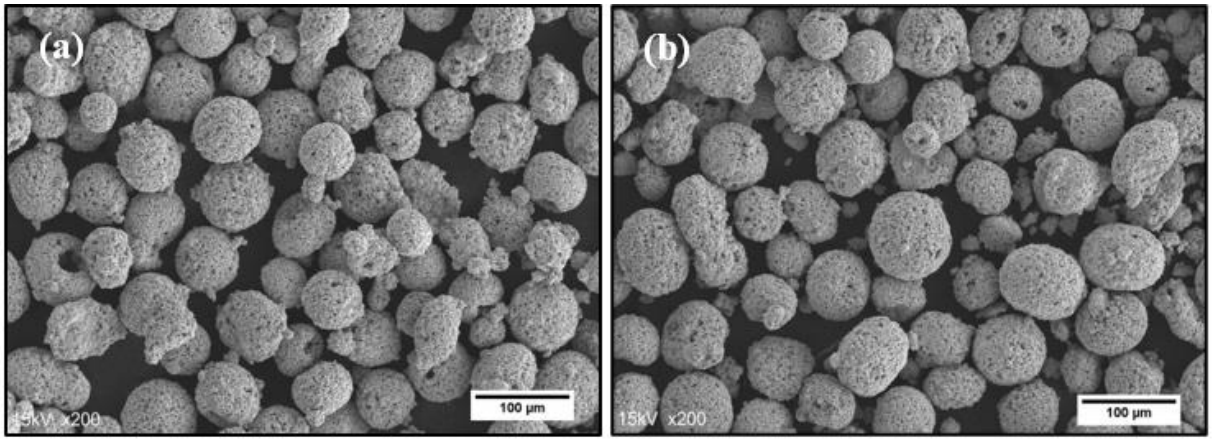

Figure 1: SEM micrographs of (a) pure Mo powder, and (b) Mo_2C powder

Substrate and its preparation method

Heat treated Forged Steel (AISI 5120) having hardness in the range of (35-40 HRC) used as a substrate with a 25 mm diameter and 5 mm thickness. This steel is mainly used for highly stressed parts with medium cross sections for automotive and general engineering applications, such as forged camshafts and gears, gear shafts, bushings and connecting rods [21]. A detailed chemical analysis of the substrate was performed using Optical Emission Spectrometer (Metal lab GNR 75/80-G, Italy) (see Table 1). Sixteen substrate samples were placed in an aluminum fixture that rotates during the spraying operation to obtain a uniform coating.
The substrate used in this study was prepared in three steps. In the first step, the substrate surface was polished and blasted with Al2O3 grits (0.6–1.4mm in diameter) to improve the adhesive bond strength between the coating and the substrate. During grit blasting, the distance between the nozzle and the substrate was kept at 100mm whereas the pressure and angle of the blasting nozzle was 5 bar and 90◦ respectively. Previous studies have shown that these parameter values produce optimized mechanical locking [22, 23]. After grit blasting the surface roughness was measured using a surface profilometer (Surfcorder-SE1700α) and it was recorded that the surface was rough to a level of ≤ 3µm from the polished surface. In the second step, samples were properly cleaned with high-pressure air to avoid any broken grit particles on the surface of the substrate, which may affect the mechanical locking of coating on the substrate. Finally, in the third step, samples were ultrasonically cleansed with acetone and alcohol.

Table 1: Chemical Composition of Aisi-5120 Used as A Substrate

Elements	Fe	C	Mn	Cr	Si	P	S
Wt.%	Base	0.21	0.89	1.25	0.24	0.017	0.015

Spraying system

After surface preparation of substrate samples, each substrate was coated with five powders (pure Mo, Mo + 10% Mo_2C, Mo + 20% Mo_2C, Mo + 30% Mo_2C and Mo + 40% Mo_2C) using atmospheric plasma spraying technique. Before spraying powder, substrates were preheated to 150◦C using a plasma gun. Temperature of substrates was noted using portable Dual laser Infra-Red pyrometer (DT-8869 H). After preheating, the powder was coated on the substrate using 3 MB plasma spraying gun. To prevent overheating in specimens during spraying, specimen holder was cooled with compressed air, and the traverse speed of the plasma spraying gun was maintained constant. Table 2 shows detailed parameters for atmospheric plasma spraying system used in this study.

Table 2: Principal Parameters Used in Atmospheric Plasma Spraying

Process parameter	Values
Current	400–650 A
Torch input power	15–30 kW
Primary gas (Argon) flow rate	40–60 L min^{-1}
Secondary gas (He) flow rate	8–15 L min^{-1}
Spraying distance	100 mm
Feed rate of the powder	25 gm. min^{-1}
Particle size	45–75 μ m

Characterization techniques

This section presents three types of characterization techniques (microstructure analysis and hardness, XRD analysis and wear testing) that were used to evaluate the quality of blended Mo-Mo_2C coatings produced using atmospheric plasma spraying technique (see Section 2.3).

Microstructural analysis and hardness

Microstructural analysis of a coating helps us to understand the morphology of the splats, their relationship with porosity, oxide contents and coating-substrate interface in the coating. On the other hand, hardness analysis of a coating helps us to determine the performance and sustainability of a coating.

Standard analytical tools were used to perform microstructural analysis and hardness on our systematically produced blended Mo-Mo_2C coatings. Optical Microscope (DM 4000 M, Leica, UK) and Scanning Electron Microscope (3700 N, Hitachi, Japan) were used to observe the spraying powder, morphology of splats, porosity and wear tracks on the coated surfaces of different sprayed systems. An image analyzer attached with an Optical Microscope was also utilized to measure the percentage porosity of the coatings.

A Vickers Micro Hardness Tester (402 MVD, Wilson) was used for micro hardness measurements of coatings as per ASTM 384. The test was performed for dwell time of 20 sec. with an applied load of 100 g on the cross sections of the coated samples and at least 5–10 readings were recorded.

X-ray diffraction analysis

To carry out XRD analysis, we used X'PERT PRO PANalytical equipped with CuKα1 (1.54Å) radiation operated at 40 mA and 40 kV. Coated samples were scanned from 20 to 120◦ 2θ with scan step size 0.02. XRD patterns were used to determine different phases in blended Mo-Mo_2C coatings, crystallite sizes of each phase and residual stresses.

Crystallite size

To estimate the crystallite size (from XRD analysis) Scherer's' formula [24] was used (see Equation 1).

$$\text{Crystallite Size} = k\,\lambda / B\,Cos\,\theta \qquad (1)$$

Where k = 0.93 is a Scherer's constant, λ = 1.54 A is the wavelength of the radiations, θ is the Bragg's angle and B is the Full Width at Half Maxima (FWHM).

To confirm the crystallite sizes of different phases formed in pure and blended Mo coatings, we used the Debye-Scherer Equation [25, 26].

Residual stresses

Residual stresses of the plasma-sprayed coatings determines the development of lattice strains, which might be due to creation of lattice defects, presence of impurity ions in the interstitial positions and thermal shocks of a substrate surface. These strains were calculated using the following formula [27].

$$\frac{\Delta d}{d} = \frac{d\,(observed) - d\,(ICSD)}{d\,(ICSD)}$$

Where $\left(\frac{\Delta d}{d}\right)$ represents the strain in the crystalline surface. The residual stresses present in the deposited coatings were calculated by multiplying strain with an appropriate value of Young's modulus of the deposited coating. [28]

Wear test

The main purpose of a wear test is to determine the wear performance of a coated material for a specific wear application. For these experiments, wear test was carried out to evaluate the tribological behavior of blended Mo-Mo_2C coatings.

For our wear test, a lab-scale ball-on-disc Tribo meter (S/N 01-02566, CSM, Switzerland) was used to measure the coefficient of friction (μ). Before wear test, samples were well polished to 0.05 μm roughness. For each sample, a fresh 100Cr3 ball of 3 mm diameter with a hardness of 64 HRC was used. Applied normal load, radius of wear track, distance travelled, and time of wear test remained constant for all five coating systems (6 N normal load, 6 mm wear track diameter, 180 m distance and 3600 s).

After wear test, samples were weighed using a balance (AUW 220D, Shimadzu) with sensitivity up to four digits in grams for measurement of weight loss during the test.

Volumetric wear loss, V_{wear}, was determined using the following equation [29]:

$$V_{wear} = \frac{mass\ loss\ (gm)}{density\ (gm/cm^3)}$$

Wear rate Kv, was calculated using the following equation [29, 30]:

$$(Wear\ Rate)\ Kv = \frac{V\ wear}{FN \times S} > \mathrm{cm^3.N^{-1}.m^{-1}}$$

Where FN is the contact load (N) and S is the sliding distance (m)

RESULTS AND DISCUSSION

This section presents the results, and their analysis obtained using three types of characterization techniques i.e. microstructure analysis and hardness, XRD analysis and wear test. Below we discuss results obtained for each characterization technique in detail.

Coating microstructures and hardness

Fig. 2 shows the Optical Micrographs of coating-substrate interfaces for pure Mo and systematically produced blended Mo-Mo_2C coatings. Overall, as expected, microstructures of all samples reveal typical lamellar structures of plasma sprayed coatings. During spraying, particles of sprayed powder move fast from the nozzle of gun and form splats, which after deformation and solidification piled up to gain the coating thickness. The Mo can form chemical bonds due its self-bonding property with many metals and alloys, however, large pores are observed in the coating as well as coating/substrate interface, resulting in weakening of adhesion strength (see Fig. 2(a). Due to the self-bonding property of Mo, when it is mixed with Mo_2C, it shows good adherence with the foreign phase (see the Optical Micrographs of Mo blended with 10%, 20%, 30% and 40% of samples in Fig. 2 (b), (c), (d) and (e), respectively). Light coloured phase is Mo and the dark colored phase is Mo_2C. There is no separation between the splats of different phases.

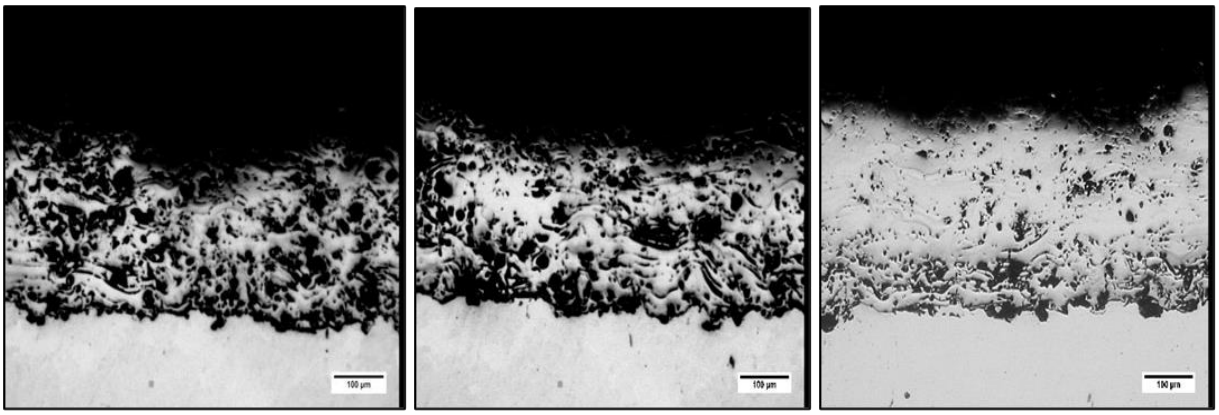

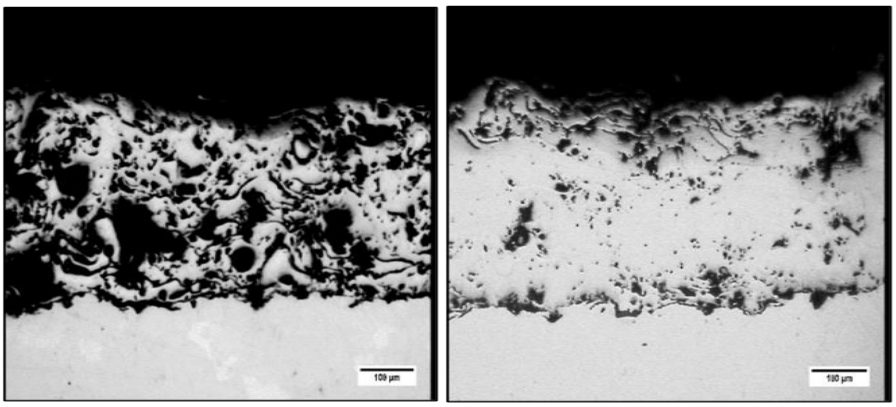

Figure 2: Optical Micrographs of coating-substrate interfaces, (a) pure Mo, (b) Mo+10%Mo_2C, (c) Mo+20%Mo_2C, (d) Mo+30%Mo_2C and (e) Mo+40%Mo_2C.

Table 3 shows results obtained for pure Mo and systematic blending of (10%, 20%, 30% and 40%) Mo_2C in pure Mo, considering thickness of splats/lamellas, porosity and hardness. Overall, our proposed combinations of blended Mo-Mo_2C coatings show better results than the pure Mo coatings (baseline) for all parameters including morphology, thickness of splats/lamellas, hardness and porosity, Among blended Mo- Mo_2C coatings, overall, best results are obtained using 40% Mo_2C in Mo. This demonstrates that blended coatings are more effective in improving microstructural and mechanical properties by decreasing the thickness of lamellas, reducing the level of porosity, oxide contents and increasing hardness than pure ones. This also highlights the fact that blending pure Mo with 40% Mo_2C is most suitable to enhance wear and friction properties of AISI 5120 material used as substrate for automobile applications.

Table 3: comparison of microstructural and mechanical properties of pure mo and blended mo-mo_2c coatings

Mo_2C Percentages	***Roughness (µm)***	***Porosity (%)***	***Cross-Sectional Hardness (HV)***	***Avg. Lamellas Thickness (µm)***	***Avg. Coating Thickness (µm)***	
0%	8.23	6.42	374	6.68	190	
10%	7.66	5.88	434.9	5.56	190	
20%	6.98	4.81	563.5	3.04	190	(±20)
30%	7.38	5.66	444.61	5.09	190	
40%	6.06	3.91	619.02	3.04	190	

Fig. 3 shows morphology and thickness of splats/lamellas observed in pure Mo and blended Mo-Mo_2C coatings. As can be noted from Fig. 3(a), pure Mo shows wide lamellas. Considering blended Mo-Mo_2C coatings (see Fig. 3 (b), (c), (d) and (e)), the thickness of lamellas decreases by addition of Mo_2C in Mo from 10% to 20%. However, as we increase the proportion of Mo_2C from 20% to 30%, thickness of lamellas also increases and it again decreases as we further increase the proportion of Mo_2C from 30% to 40%. As expected, with a change in the thickness of lamellas/splats, the porosity also changes.

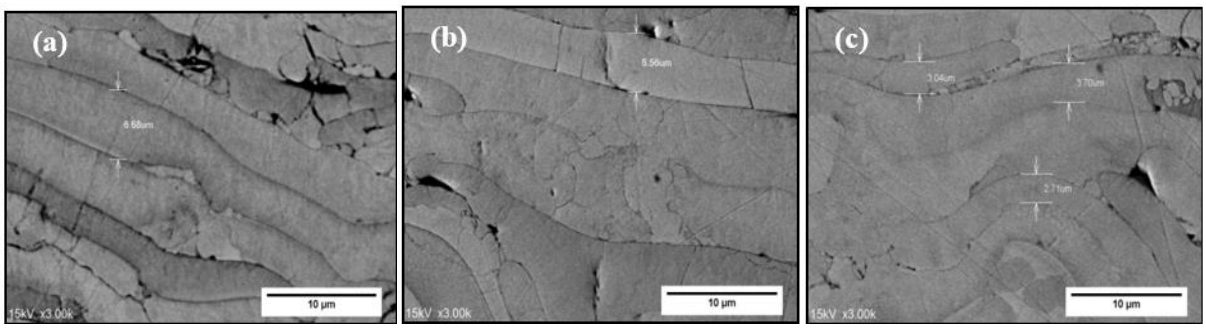

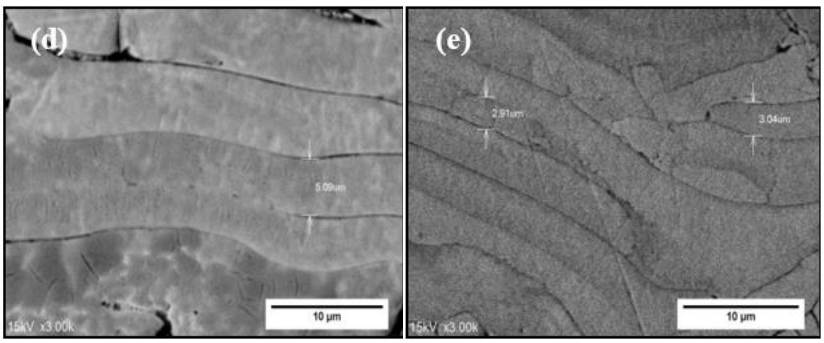

Figure 3: SEM Micrographs showing morphology of lamellas, (a) Mo, (b) Mo+10%Mo_2C, (c) Mo+20%Mo_2C, (d) Mo+30%Mo_2C and (e) Mo+40%Mo_2C.

Regarding porosity, best results are obtained using blended coatings (Mo+ 40%Mo_2C). As can be noted from Table 4, worst results are obtained using pure Mo. The possible reason is that the Mo powder in the plasma jet transforms to the molten state with a low degree of melting due to its high melting point, which results in high porosity due to occurrence of low degree of deformation on the surface of substrate during solidification (see Fig. 3(a)). Considering blended Mo-Mo_2C coatings (see Fig. 3 (b), (c), (d) and (e)), an interesting trend is observed that the porosity level decreases on addition of Mo_2C from 10% to 20%. However, as we increase the proportion of Mo_2C from 20% to 30% the porosity level increases and it again decreases as we further increase Mo_2C from 30% to 40%. This shows that we have an almost same trend in porosity from 10% Mo_2C to 20% Mo_2C and 30% Mo_2C to 40% Mo_2C in pure Mo. Fig. 5 shows effect of Mo_2C addition on the microstructures and percentage porosity. As can be noted from this figure that addition of Mo_2C can effectively reduce porosity of pure Mo. These results clearly show that value of porosity of pure Mo coated samples is 6.42%. By adding 10% of Mo_2C, porosity of blended coating drops to 5.88%. It further drops to 4.81% for 20% Mo_2C, but it increases to 5.66% for 30% Mo_2C and again drops to 3.91% for 40% Mo_2C.

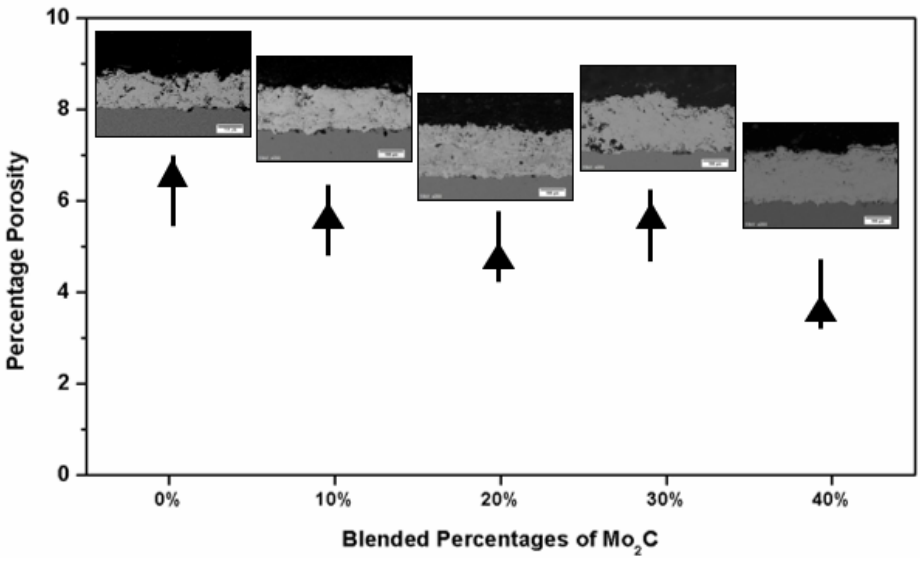

Figure 4: Effect of Mo_2C addition on microstructures and percentage porosity

Regarding formation of oxides, presence of Mo_2C lowers the formation of oxides, while some oxides may be expected to form during the high temperature process (such as MoO_2) as shown in Fig. 2 (this is also confirmed by the XRD results presented in the next section). As can be noted from Fig. 2 that oxide contents are very low and SEM images show irregular structures of these oxides (see Fig. 5). Note that the quantities of oxide contents presented here are estimates because it is not possible to accurately compute the quantities of these oxide contents using an image analyzer [31].

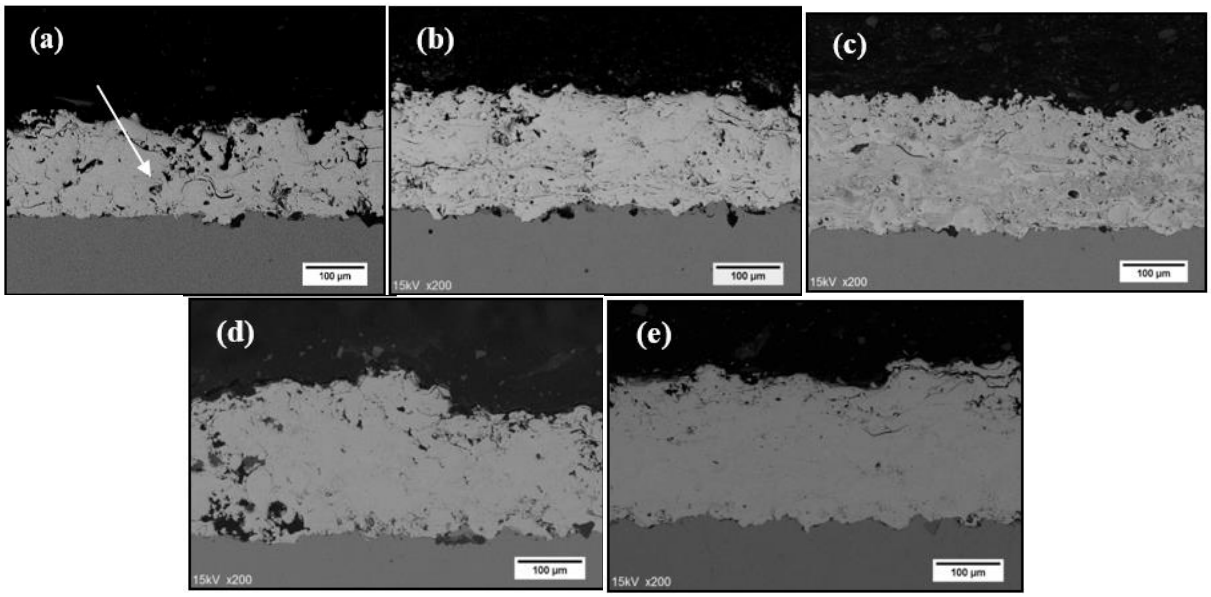

Figure 5: SEM Micrographs of coating-substrate interfaces, (a) pure Mo, (b) Mo+10%Mo_2C, (c) Mo+20%Mo_2C, (d) Mo+30%Mo_2C and (e) Mo+40%Mo_2C.

Table 4 shows hardness values for pure Mo and Mo-Mo_2C blended coatings. As can be noted from these results that hardness of blended coatings varies with the proportions of Mo_2C. These results also demonstrate that hardness of coatings is related with percentage porosity as well as morphology and thickness of lamellas. In this study, we obtained hardness value of 368 HV for pure Mo coatings. Note that this hardness value is consistent with previously reported ones [12, 19]. As the amount of Mo_2C increases from 10% to 20%, the level of porosity decreases, and the coating hardness increases (see Fig.6). However, as we increase Mo_2C from 20% to 30%, hardness decreases and on further increase of Mo_2C from 30% to 40%, the level of hardness increases.

To conclude, microstructures and hardness analysis shows that compared to pure Mo coating (baseline) our proposed blended coatings (Mo + 20% Mo_2C and Mo + 40% Mo_2C) show better results in improving morphology of splats/lamellas, level of porosity, oxide contents and hardness. This demonstrates the fact that same wear properties are obtained using small (10% to 20%) and large (30% to 40%) percentages of Mo-Mo_2C blended coatings. As discussed earlier (see Section 1), in contrast to previous studies on blended coatings (which used a random single percentage for blending) [32], our proposed study is systematic with four percentage variations at an interval of 10%. Previous studies failed to reveal this pattern of similar performance at small and large percentages of blending. Consequently, we can say that our proposed methodology of systematic blending is more useful and effective than previously reported methodologies which just use a random percentage for blending.

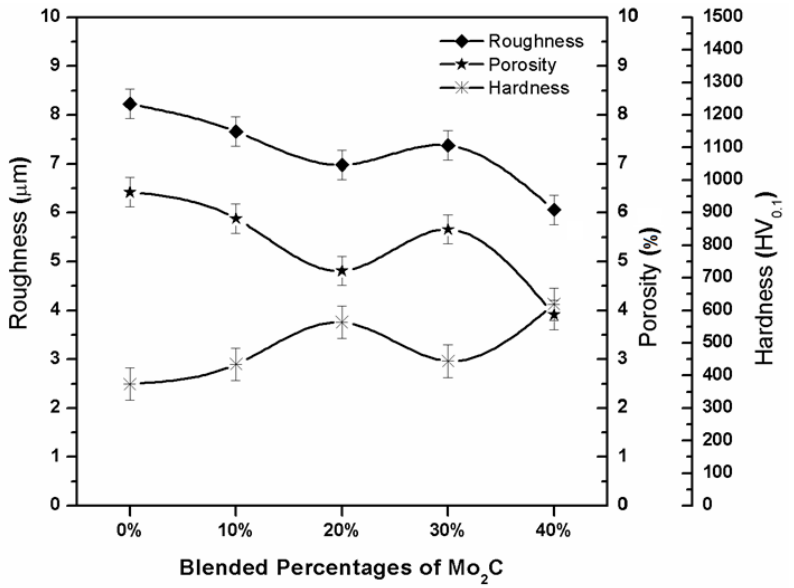

Figure 6: Relationship between roughness, porosity and hardness of pure Mo and blended Mo-Mo_2C coatings

X-ray Diffraction analysis

Fig. 7 shows XRD patterns of coated samples of pure Mo and four blends of Mo with 10%,20%,30%and 40% of Mo_2C in the range of $2\theta = 20°–120°$. The reflections are matched well with the reported values in the standard powder diffraction files having Nos. 03-065-7442, 01-077-0720, 03-065-1273 and 01-072-0527 which corresponds to Mo, Mo_2C, MoO_2 and Mo_3O phases respectively.

XRD analysis shows presence of MoO_2 on the surface of coated samples of pure Mo due to oxidation of Mo at high temperature of atmosphere plasma spraying process. When Mo_2C is added in pure Mo with four percentage variations, then oxidation of Mo reduces due to sacrificial role of carbon present in carbides form. Similarly, content of retained Mo_2C also increases on higher percentages of 30% and 40%. The Mo peaks in XRD graph are showing a visible shift from left to right as proportion of Mo_2C increases from 10% to 20%. The same trend is observed on increasing this proportion from 30% to 40%. Mo_2C.

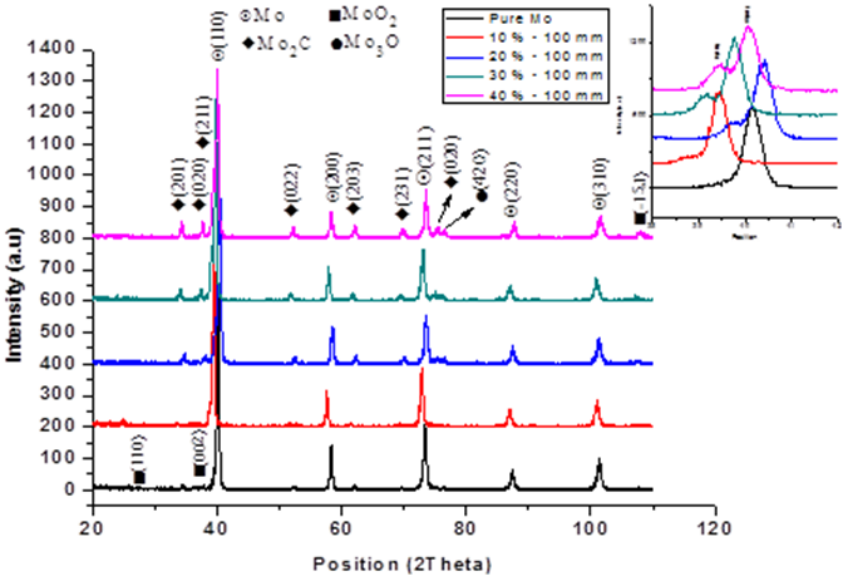

Figure 7: XRD spectra for pure Mo and blended Mo with Mo_2C

Crystallite size

Fig. 8(a) shows the crystallite sizes of Mo phase in pure Mo which varies from 30–90 nm. On the other hand, by varying the proportion of Mo_2C, from 10% to 20%, crystallite sizes vary from 40 – 90 nm to 30–75 nm and from 30% to 40%, crystallite sizes vary from 30– 80 nm to 30–70 nm.

Fig. 8(b) shows crystallite sizes of Mo_2C distributed in matrix of pure Mo. As can be noted from this figure that by varying percentage of Mo_2C from 10% to 20%, crystallite sizes vary from 50–95 nm to 50– 110 nm and when we vary percentage of Mo_2C from 30% to 40%, crystallite sizes vary from 50–100 nm to 50–90 nm. Considering crystallite sizes of MoO_ and Mo_3O, as we change percentage of Mo_2C from 10% to 20% and 30% to 40%, crystallite sizes vary from 40–90 nm and 60–40 nm respectively. For Mo_3O, crystallite sizes vary from 60–80 nm and it remains same at 20% and 40% of Mo_2C (seeFig.8(c)).

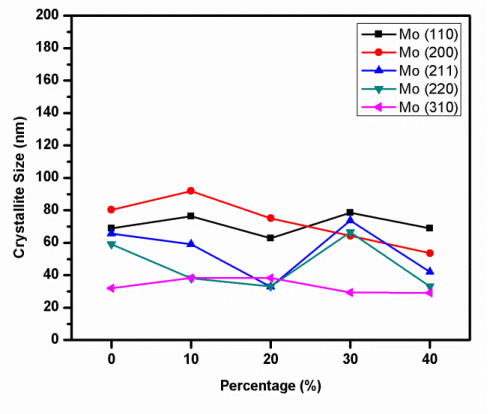

(a)

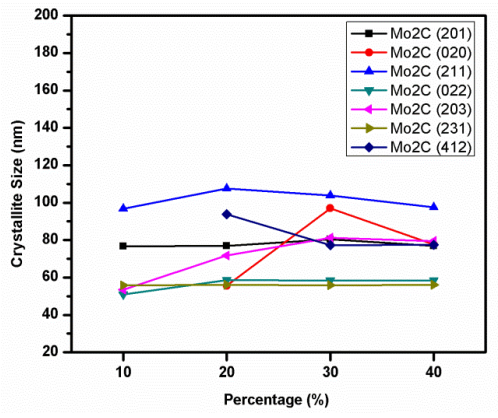

(b)

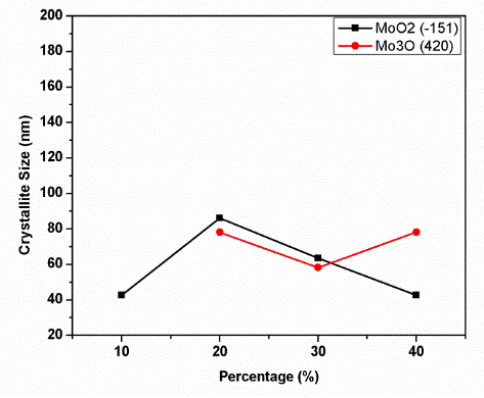

(c)

Figure 8: Crystallite size of phases: (a) Mo (b) Mo_2C (c) MoO_2 and Mo_3O

Residual stresses

Fig. 9(a), (b) and (c) show behavior of residual stresses developed in different phases of Mo, Mo_2C, MoO_2 and Mo_3O in pure Mo and blended Mo-Mo_2C coatings. From Fig. 3(a), it can be noted that Mo phase in pure Mo coated samples shows compressive stresses. Considering blended Mo-Mo_2C coatings, for Mo + 10%Mo_2C blended coatings, Mo and other phases Mo_2C, MoO_2 and Mo_3O show tensile stresses. For Mo + 20% Mo_2C blended coatings, Mo phase shows negligible stress level and other phases, Mo_2C, MoO_2 and Mo_3O are showing compressive stresses. Similarly, same trend is observed at Mo + 30%Mo_2C and Mo + 40%Mo_2C blended coatings in which tensile stresses are changing to compressive stresses.

To conclude, XRD analysis of coatings produced by systematically blending Mo_2C with pure Mo using atmospheric plasma spraying shows that residual stresses are related to crystallite sizes of different phases developed in pure Mo and blended Mo-Mo_2C coatings. It is also observed that as the crystallite sizes of phases are reduced, phases show compressive stresses and it improves mechanical and tribological properties of blended Mo-Mo_2C coatings. On the other hand, if crystallite sizes increase then phases show tensile stresses and it reduces mechanical and tribological properties of blended Mo-Mo_2C coatings. Relationship between residual stresses and wear rate of blended Mo-Mo_2C coatings can be explained on the basis of magnitude of these residual stresses. We observe that Mo and Mo_2C phases in Mo+10%Mo_2C and Mo+30%Mo_2C show tensile stresses whereas in case of Mo+20%Mo_2C and Mo+40%Mo_2C, it changes to compressive stresses. It is evident from literature that compressive stresses improve the mechanical properties of the surface of the coating. [33] Whereas wear rate decreases with increase in compressive stresses within the coating [34]. Therefore, decrease in wear rate for the coating systems (Mo+20%Mo_2C and Mo+40%Mo_2C) is subjected to high compressive stresses.

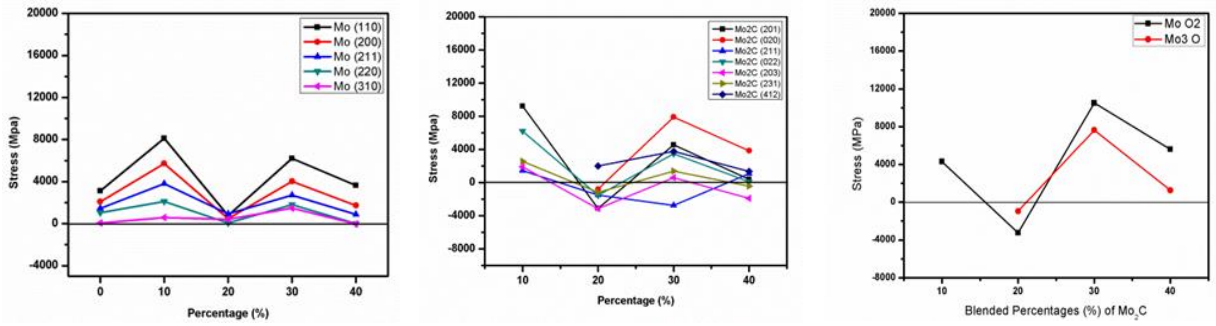

(a) (b) (c)

Figure 9: Stress graph of phases: (a) Mo (b) Mo_2C (c) MoO_2 and Mo_3O

Wear test

Table 4 shows results obtained for pure Mo and blended Mo-Mo_2C coatings for the wear test. Overall, results show that change in wear rate of blended Mo-Mo_2C coating system is subjected to the addition of harder and more brittle Mo_2C phase in Mo matrix, because the strengthening mechanism of different coating systems directly affects change in wear and friction properties of blended coatings. It is quite apparent that increase in Mo_2C is related to wear mechanism and wear mechanism is a key factor governing wear rate of coatings.

In wear testing, mechanism of wear for pure Mo and blended Mo-Mo_2C coatings is used to explain the test results. An overall results show that wear rate is directly related with coefficient of friction of coated samples. Fig. 9 shows relationship between wear rate and coefficient of friction. It can be observed from this figure that wear rate is directly

proportional to coefficient of friction. As coefficient of friction of blended Mo-Mo_2C coatings decreases, wear rate also decreases. Similarly, when values of coefficient of friction increases, wear rate also increases.

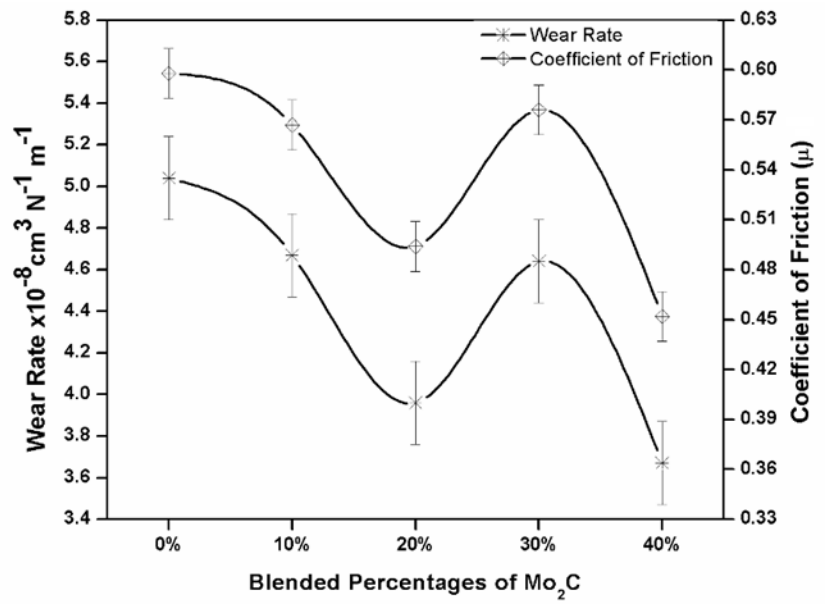

Figure 10: Relationship between wear rate and coefficient of Friction of pure and blended Mo with Mo_2C

For example, as percentage of Mo_2C in Mo increases from 10% to 20%, the value of coefficient of friction decreases from 0.598 to 0.580μm, which decreases the value of wear rate from 4.67 to 3.96 $\times 10^{-8}cm^3N^{-1}m^{-1}$. As percentage of Mo_2C changes from 20% to 30%, value of coefficient of friction increases from 0.580 to 0.525μm, which increases the value of wear rate from 3.96 to 4.64$\times 10^{-8}cm^3N^{-1}m^{-1}$. Similarly, when percentage Mo_2C changes from 30% to 40%, value of coefficient of friction decreases from 0.525 to 0.494μm and value of wear rate decreases from 4.64 to 3.67$\times 10^{-8}cm^3N^{-1}m^{-1}$ as shown in Table 4.

Table 4: Comparison Of Wear Rate and Coefficient of Friction of Blended Molybdenum Coatings

Mo_2C Percentages	**0%**	**10%**	**20%**	**30%**	**40%**
*Wear Rate**	5.04	4.67	3.96	4.64	3.67
C.O.F (μ)	0.644	0.598	0.58	0.525	0.494

*$\times 10^{-8}cm^3N^{-1}m^{-1}$

Fig.11 shows a clear change in surface morphology of coatings after wear test due to variation of wear scars. It can be observed that pure Mo coated sample has a maximum worn surface (see Fig.11 (a)), whereas with an increase in percentage of Mo_2C from 10% to 40% in pure Mo (see Figs. 11(b), (c), (d) and (e)), wear scars become minimal. Observations of worn surfaces can be related to coating microstructures (see Section 2.4.1); that are directly related to the percentage porosity of the blended Mo-Mo_2C coating. Results show that the blended Mo-Mo_2C coating with 40% Mo_2C show the lowest percentage of porosity, having least wear scars and a less wear rate.
Similarly, pure Mo coating shows highest percentage of porosity, having maximum number of wear scars and a maximum wear rate.

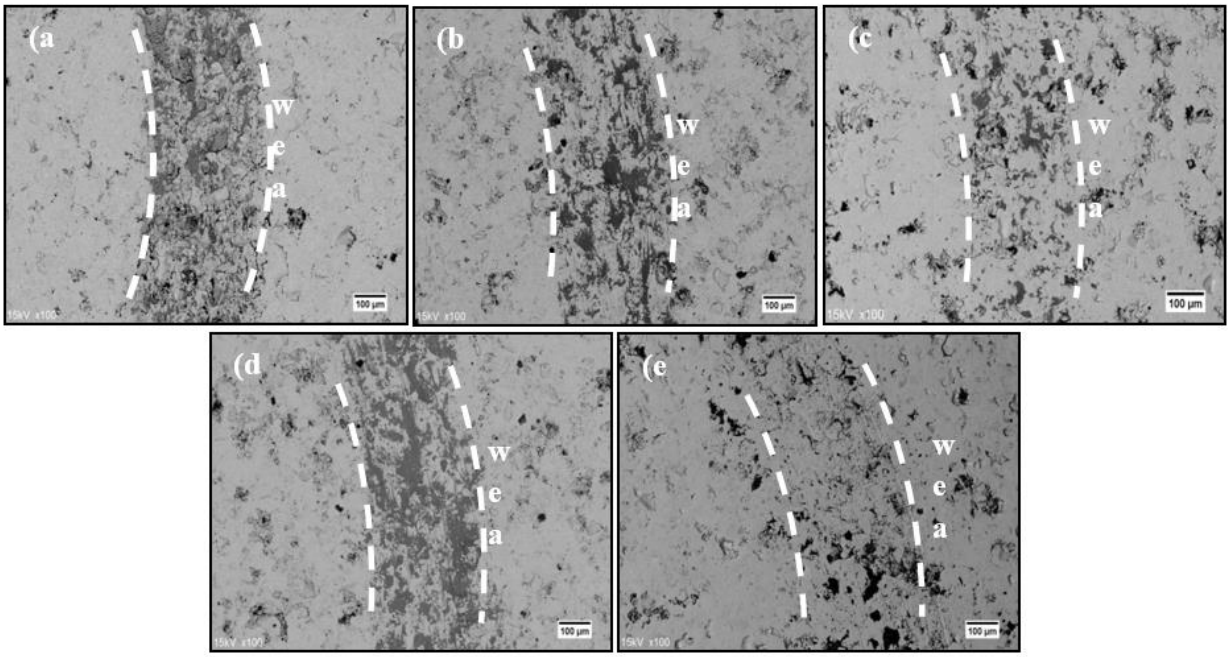

Figure 11: Surface morphology of coatings: (a) Pure Mo, (b) 10% Mo_2C, (c) 20% Mo_2C, (d) 30% Mo_2C, and (e) 40% Mo_2C after the wear test, demonstrating the variation in wear scar

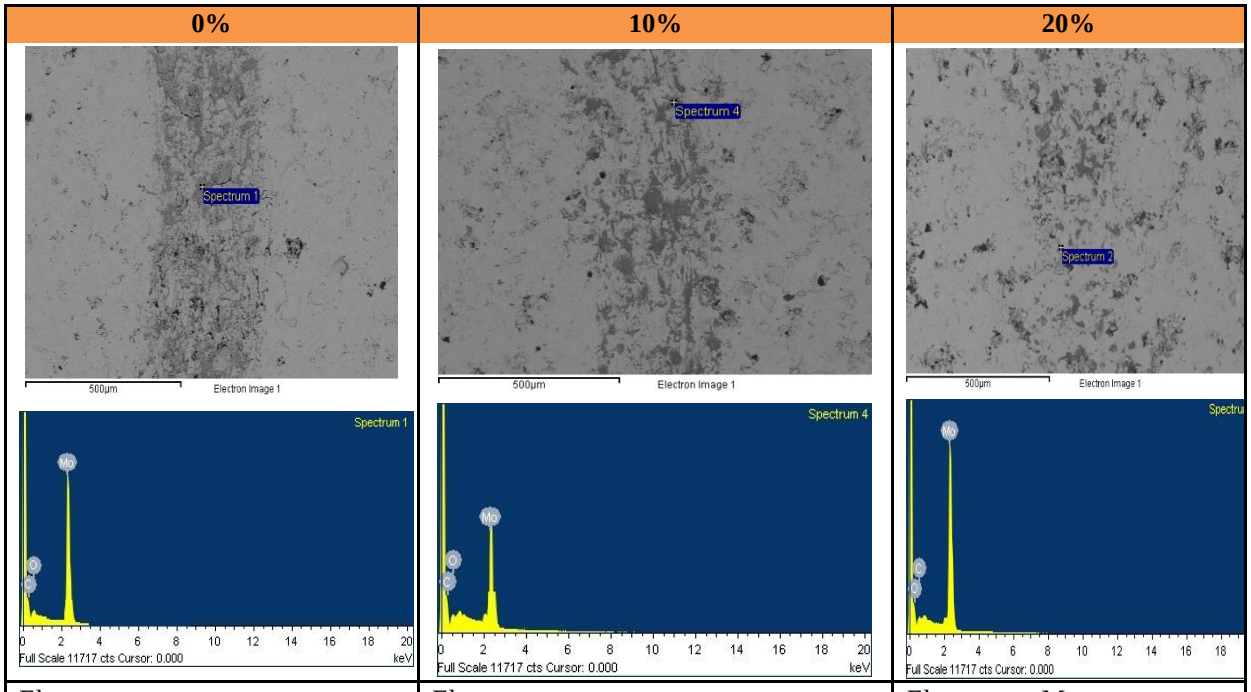

0%				10%				20%			
Elements	Mo	O	C	Elements	Mo	O	C	Elements	Mo	O	C
Weight %	66.0	33.2	0.8	Weight %	70.8	16.6	12.6	Weight %	82.0	3.6	14.4

30%	40%

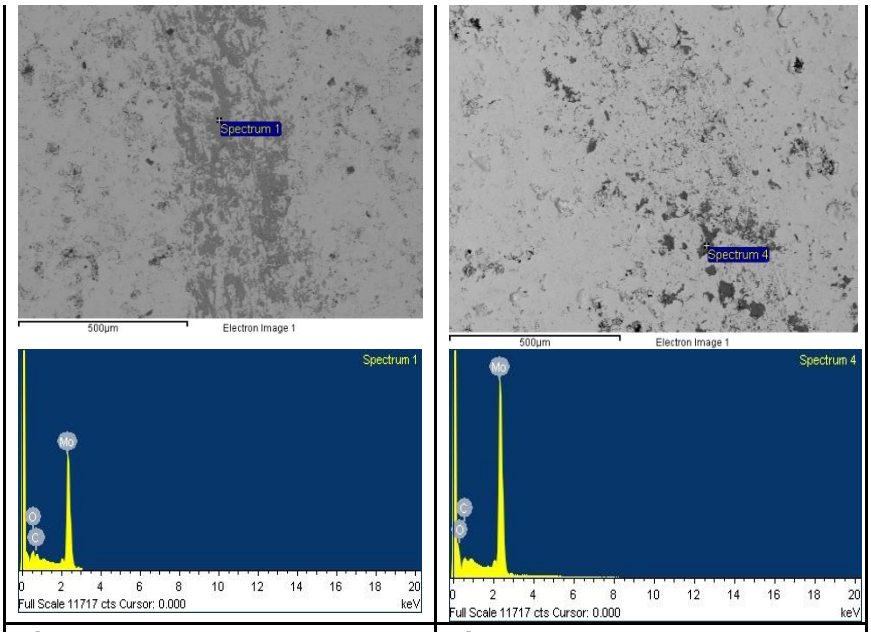

Elements	Mo	O	C
Weight %	75.4	12.7	11.9

Elements	Mo	O	C
Weight %	83.8	2.21	13.99

Figure 12: SEM-EDX analysis of coatings: (a) Pure Mo, (b) 10% Mo_2C, (c) 20% Mo_2C, (d) 30% Mo_2C, and (e) 40% Mo_2C after the wear test

CONCLUSION

The two main findings of this study are as follows. Firstly, the wear performance of blended Mo-Mo_2C coatings is dependent on the wear mechanism of the coating, which in turn, depends on the proportion of Mo and Mo_2C phases within the coating. Secondly, the amount of Mo_2C plays an important role for the tribological behavior of Mo-Mo_2C coatings. When the amount of Mo_2C is low, cracking and delamination of Mo_2C splats is more due to inadequate mechanical locking provided by Mo. whereas if the amount of Mo_2C is high, the strong structure of Mo_2C can provide the required wear resistance resulting in lower wear damage of coating.

REFERENCES

[1]. Chattopadhyay, R. Advanced thermally assisted surface engineering processes. Springer Science & Business Media (2004)
[2]. Chattopadhyay, R. Surface wear: analysis, treatment, and prevention. ASM international (2001)
[3]. Pawlowski, L. The science and engineering of thermal spray coatings. John Wiley & Sons. (2008)
[4]. Kusoglu, I. M., Celik, E., Cetinel, H., Ozdemir, I., Demirkurt, O., & Onel, K. Wear behavior of flame-sprayed Al2O3–TiO2 coatings on plain carbon steel substrates. Surface and Coatings Technology. 200(1): 1173-1177 (2005)
[5]. Yılmaz, Ş. 2009.An evaluation of plasma-sprayed coatings based on Al2O3 and Al2O3–13wt. % TiO2 with bond coat on pure titanium substrate. Ceramics International. 35(5): 2017-2022.
[6]. Mohseni, M., Ramezanzadeh, B., Yari, H., & Gudarzi, M. M. The role of nanotechnology in automotive industries. INTECH Open Access Publisher (2012)
[7]. Laribi, M.; Vannes, A.B.; Treheux, D. Study of Mechanical Behavior of Molybdenum Coating Using Sliding Wear and Impact Tests. Wear, 262, 1330–1336 (2007)
[8]. Farahmand, R.; Sohrabi, B.; Ghaffarinejad, A.; Meymian, M.R.Z. Synergistic effect of molybdenum coating and SDS surfactant on corrosion inhibition of mild steel in presence of 3.5% NaCl. Corros. Sci., 136, 393–401 (2018)
[9]. Osadnik, M.; Wrona, A.; Lis, M.; Kami´ nska, M.; Bilewska, K.; Czepelak, M.; Czechowska, K.; Moskal, M.; Wi˛ecław, G. Plasma-sprayed Mo-Re Coatings for Glass Industry Applications. Surf. Coat. Technol. 318, 349–354 (2017)
[10]. Sampath, S., Usmani, S., & Houck, D. L. Applications of Mo and Mo-alloys as thermal spray coatings. Minerals, Metals and Materials Society/AIME:Molybdenum and Molybdenum Alloys (USA). 145-154 (1998)

[11]. Tura, J. M., Traveria, A., De Castellar, M. D., Pujadas, J., Blouet, J., Gras, R., & Romero, A. Frictional properties and wear of a molybdenum coating and a bronze (Cu-10% Sn) with friction modifier fillers. Wear. 189(1): 70-76 (1995)
[12]. Ahn, J., Hwang, B., & Lee, S. Improvement of wear resistance of plasma-sprayed molybdenum blends coatings. Journal of thermal spray technology. 14(2): 251-257 (2005)
[13]. Hwang, B.; Ahn, J.; Lee, S. Effects of Blending Elements on Wear Resistance of Plasma-Sprayed Molybdenum Blend Coatings Used for Automotive Synchronizer Rings. Surf. Coat. Technol. 194, 256–264 (2005)
[14]. Yan, J.H.; He, Z.Y.; Wang, Y.; Qiu, J.W.; Wang, Y.M. Microstructure and Wear Resistance of Plasma-sprayed Molybdenum Coating Reinforced by MoSi2 Particles. J. Therm. Spray Technol. 26, 1322–1329. [Cross Ref] (2016)
[15]. Prchlik, L.; Gutleber, J.; Sampath, S. Deposition and Properties of High-Velocity-Oxygen-Fuel and Plasma-Sprayed Mo-Mo_2C Composite Coatings. J. Therm. Spray Technol. 10, 643–655. [Cross Ref]-(2001)
[16]. Debasish, D.;Mantry, S.; Behera, D.; Jha, B.B. Improvement of Microstructural and Mechanical Properties of Plasma Sprayed Mo Coatings Deposited on Al-Si Substrates by Premixing of Mo with TiN Powder. High Temp. 52, 19–25 (2014)
[17]. Liao, J., Wilcox, R. C., & Zee, R. H. Structures and properties of the Mo- Mo_2C system. Scripta Metallurgica et Materialia.24(9): 1647-1652. (1990)
[18]. Sampath, S., & Wayne, S. F. Microstructure and properties of plasma-sprayed Mo-Mo_2C composites. Journal of Thermal Spray Technology. 3(3): 282-288 (1994)
[19]. Rastegar, F., & Craft, A. E. Piston ring coatings for high horsepower diesel engines. Surface and Coatings Technology. 61(1): 36-42 (1993)
[20]. Hwang, B., Lee, S., & Ahn, J. Correlation of microstructure and wear resistance of molybdenum blend coatings fabricated by atmospheric plasma spraying. Materials Science and Engineering: A, 366(1), 152-163 (2004)
[21]. https://www.steelforge.com/alloy-steel-aisi-5120/
[22]. Staia, M. H., Ramos, E., Carrasquero, A., Roman, A., Lesage, J., Chicot, D.,and Mesmacque,G. "Effect of Substrate Roughness Induced by Grit Blasting upon Adhesion of WC-17%Co Thermal Sprayed Coatings," Thin Solid Films, 377–378, pp 657–664. (28)- (2000)
[23]. Gadow, R., Candel, A., and Floristan, M. "Optimized Robot Trajectory Generation for Thermal Spraying Operations and High Quality Coatings on Free-Form Surfaces," Surface and Coatings Technology, 205(4), pp 1074–1079 (2010)
[24]. K. Nordlund, M. Ghaly, R.S. Averback, M. Caturla, T. Diaz de la Rubia and Tarus, J. Phys. Rev. B 57, 7556 (1998)
[25]. Latif, A., Rehman, M. K., Rafique, M. S., Bhatti, K. A., and Imran, M. "Irradiation Effects on Copper," Radiation Effects and Defects in Solids, 164(1), pp 68–72 (2009)
[26]. Latif, A., Rehman, M. K., Bhatti, K. A., Rafique, M. S., and Rizvi, Z. H. "Crystallography and Surface Morphology of Ion-Irradiated Silver," Radiation Effects and Defects in Solids, 164(4), pp 265–271 (2011)
[27]. C. S. Chen, C. P. Liu, C. Y. A. Tsao, Thin Solid Films 479 -130 (2005)
[28]. Nino, A., Takahashi, N., Sugiyama, S., & Taimatsu, H. Effects of carbide grain growth inhibitors on the microstructures and mechanical properties of WC–SiC–Mo_2C hard ceramics. International Journal of Refractory Metals and Hard Materials, 43, 150-156 (2014)
[29]. Espinosa, L., Bonache, V., and Salvador, M. D. "Friction and Wear Behavior of WC-Co-Cr3C2-VC Cemented Carbides Obtained from Nano crystalline Mixtures," Wear, 272(1), pp 62–68 (2011)
[30]. Pirso, J., Viljus, M., and Letunovits, S. "Friction and Dry Sliding Wear Behavior of Cermets," Wear, 260(7–8), pp 815–824 (2006)
[31]. Niranatlumpong, P., & Koiprasert, H. The effect of Mo content in plasma-sprayed Mo-NiCrBSi coating on the tribological behavior. Surface and Coatings Technology, 205(2), 483-489 (2010)
[32]. Yan, J., Guo, Y., Wang, Y., Zhou, P., & Qiu, J. A Comparison Study on Wear Behaviors of Mo and Al2O3-Mo Coatings from RT to 300° C. Lubricants, 6(2), 48 (2018)
[33]. Montay, G., Cherouat, A., Nusair, A., and Lu, J. "Residual Stresses in Coating Technology," Journal of Materials Science &Technology, 20(1), pp 81–84 (2004)
[34]. Afzal, M., Ajmal, M., & Khan, A. N. Wear behavior of WC-12% Co coatings produced by air plasma spraying at different standoff distances. Tribology Transactions, 57(1), 94-103 (2014)